

N-glycosylation by N-acetylglucosaminyltransferase V enhances the interaction of CD147/basigin with integrin β 1 and promotes HCC metastasis

Jian Cui^{1†}, Wan Huang^{1†}, Bo Wu^{2†}, Jin Jin¹, Lin Jing¹, Wen-Pu Shi¹, Zhen-Yu Liu¹, Lin Yuan¹, Dan Luo¹, Ling Li¹, Zhi-Nan Chen^{1*} and Jian-Li Jiang^{1*}

¹ Cell Engineering Research Centre and Department of Cell Biology, State Key Laboratory of Cancer Biology, Fourth Military Medical University, Xi'an, PR China

² State Key Laboratory of Proteomics, Beijing Proteome Research Center, Beijing Institute of Radiation Medicine, Collaborative Innovation Center for Cancer Medicine, Beijing, PR China

*Correspondence to: Jian-Li Jiang or Zhi-Nan Chen, Cell Engineering Research Centre and Department of Cell Biology, State Key Laboratory of Cancer Biology, Fourth Military Medical University, 169 Chang le West Road, Xi'an, 710032, PR China. E-mail: jiangjl@fmmu.edu.cn; zhinanchen@fmmu.edu.cn

†These authors contributed equally to this work.

Abstract

While the importance of protein N-glycosylation in cancer cell migration is well appreciated, the precise mechanisms by which N-acetylglucosaminyltransferase V (GnT-V) regulates cancer processes remain largely unknown. In the current study, we report that GnT-V-mediated N-glycosylation of CD147/basigin, a tumor-associated glycoprotein that carries β 1,6-N-acetylglucosamine (β 1,6-GlcNAc) glycans, is upregulated during TGF- β 1-induced epithelial-to-mesenchymal transition (EMT), which correlates with tumor metastasis in patients with hepatocellular carcinoma (HCC). Interruption of β 1,6-GlcNAc glycan modification of CD147/basigin decreased matrix metalloproteinase (MMP) expression in HCC cell lines and affected the interaction of CD147/basigin with integrin β 1. These results reveal that β 1,6-branched glycans modulate the biological function of CD147/basigin in HCC metastasis. Moreover, we showed that the PI3K/Akt pathway regulates GnT-V expression and that inhibition of GnT-V-mediated N-glycosylation suppressed PI3K signaling. In summary, β 1,6-branched N-glycosylation affects the biological function of CD147/basigin and these findings provide a novel approach for the development of therapeutic strategies targeting metastasis.

© 2018 The Authors. *The Journal of Pathology* published by John Wiley & Sons Ltd on behalf of Pathological Society of Great Britain and Ireland.

Keywords: N-glycosylation; basigin; EMMPRIN; CD147; metastasis; protein–protein interaction; epithelial to mesenchymal transition

Received 20 October 2017; Revised 28 January 2018; Accepted 6 February 2018

No conflicts of interest were declared.

Introduction

Accumulating evidence shows that aberrant glycosylation occurs frequently in cancer [1,2]. Alterations in glycosylation patterns regulate cancer development and progression, serve as important biomarkers, and provide a set of specific targets for diagnosis and therapeutic intervention [3–6]. The modifications most often associated with cancer include sialylation, β 1,6-GlcNAc-branched N-glycans, and core fucosylation [7]. Increased GlcNAc-branched N-glycan levels result from increased activity of N-acetylglucosaminyltransferase V (GnT-V) encoded by the mannoside acetylglucosaminyltransferase 5 (MGAT5) gene and are closely associated with cancer metastasis [8]. For example, an increase in GnT-V-dependent N-glycan modifications enhances the

invasiveness of glioma, colon cancer, and gastric cancer cells by regulating cell adhesion [1,9], whereas core fucosylation, catalyzed by fucosyltransferase VIII, is involved in the expression of cancer biomarkers [10].

CD147, also known as basigin or EMMPRIN, is a tumor-associated transmembrane glycoprotein that belongs to the immunoglobulin superfamily [11–13]. As an extracellular inducer of MMPs, basigin is aberrantly expressed on the cell surface of various tumors and correlates with aggressive disease and poor prognosis [12,14,15]. In hepatocellular carcinoma (HCC), CD147/basigin is closely associated with carcinogenesis, EMT, and chemoresistance [16–19]. Mature CD147/basigin is highly glycosylated; N-glycosylation accounts for almost half of the molecular weight [20,21]. CD147/basigin contains three N-linked glycosylation sites (Asn44, Asn152, and Asn186), which contribute

to both the high-glycosylated form (~40–60 kDa) and the low-glycosylated form (~32 kDa) [22,23]. Despite previous work, the contribution of glycans to CD147/basigin function remains unknown [24,25].

Here, we report the clinical relevance of CD147/basigin- β 1,6-branching in HCC and show that β 1,6-GlcNAc glycans are required for CD147/basigin to induce EMT and maintain the aggressiveness and malignant properties of HCC. In addition, we found that the PI3K/Akt pathway regulates GnT-V-mediated *N*-glycosylation in HCC cells. With these data, we propose a model to explain how GnT-V-mediated glycosylation of CD147/basigin promotes HCC metastasis.

Materials and methods

Patients

Sixty-five HCC patients were recruited from the Eastern Hepatobiliary Hospital affiliated with The Second Military Medical University (Shanghai, China), and these patients provided written informed consent. Ethical approval for experiments involving human samples was granted by the Ethics Committee of The Fourth Military Medical University, and all experimental protocols were conducted in accordance with the relevant guidelines and regulations.

Cell culture and plasmids

Human HCC (HepG2), human normal hepatic (QZG), and human embryonic kidney (HEK293T) cells were obtained from the Institute of Cell Biology of the Chinese Academy of Sciences (Shanghai, China). The human HCC cell line (Huh-7) was obtained from the Japanese Collection of Research Bioresources (JCRB, Osaka, Japan). QZG and HEK293T cells were cultured in RPMI 1640 medium (Gibco, New York, NY, USA); HepG2 and Huh-7 cells were cultured in DMEM. All media were supplemented with 10% fetal bovine serum, 2 mM glutamine, 100 μ g/ml penicillin, and 100 μ g/ml streptomycin, and cells were incubated at 5% CO₂ and 37 °C. All cells were authenticated by short tandem repeat profiling. The plasmids WT-eGFP-N1-CD147 and N44Q/N152Q/N186Q (3Q)-eGFP-N1-CD147 were used as described previously [22].

Antibodies, immunohistochemical staining, and reagents

Antibody details are listed in the supplementary material, Table S1. Rabbit anti-CD147 and α -tubulin were developed in our laboratory [26]. Formalin-fixed, paraffin-embedded tissues from HCC patients were stained with HAb18G antibody against CD147 (30 μ g/ml) and PHA-L (1:200) for β 1,6-branched *N*-glycans as previously described [15]. The PI3K inhibitor LY294002 was purchased from Cell Signaling Technology (Danvers, MA, USA). TGF- β 1 (100-210) was purchased from PeproTech (Rocky Hill, NJ, USA)

and swainsonine (s9263) from Sigma-Aldrich (St Louis, MO, USA).

In situ proximity ligation assay (PLA)

Duolink® *In Situ* Detection Reagents Red (Sigma-Aldrich) were used according to the manufacturer's instructions. Rabbit anti-CD147 (10 μ g/ml) and biotinylated PHA-L (1:200) were applied overnight at 4 °C, followed by mouse anti-biotin. The PLA probes used were anti-mouse immunoglobulin PLUS and anti-rabbit-MINUS. Images were acquired using a fluorescence microscope, and PLA signals were analyzed with the Duolink ImageTool (Sigma-Aldrich).

siRNA transfection

Silencing was accomplished by transient transfection of siRNA oligonucleotides using Lipofectamine 2000 (Invitrogen, Carlsbad, CA, USA) following the manufacturer's instructions. We employed a pool of four RNAi oligonucleotides for *MGAT5* (ON-TARGET plus, Dharmacon Smart Pool library, Lafayette, CO, USA), and an oligonucleotide from GenePharma (Shanghai, China) was used as the negative control (supplementary material, Table S2).

Immunofluorescence

Immunofluorescence was performed as previously described [19], but without detergent treatment. Briefly, actively growing Huh-7 and HepG2 cells (5×10^4) were seeded into dishes pre-coated with 1% Matrigel (BD Biosciences, San José, CA, USA) and cultured overnight before being fixed with 4% paraformaldehyde and then blocked with 3% BSA in PBS for 0.5 h. Cells were incubated overnight with a mixture of biotinylated PHA-L (1:200), mouse anti-biotin, and rabbit anti-CD147 (10 μ g/ml); washed in PBS; and incubated with secondary fluorescent antibodies in PBS for 3 h. Nuclei were counterstained with DAPI (1:50 dilution; Vector Laboratories, Burlingame, CA, USA) and samples were visualized with a confocal microscope using Nikon NIS-Elements software (Nikon, Tokyo, Japan).

In vitro invasion assays

Huh-7 cells (5×10^4) were seeded onto Matrigel (BD Biosciences) in chambers (Merck Millipore, Darmstadt, Germany) inserted into 24-well plates. Cell invasion was evaluated after 48 h using an inverted phase-contrast microscope. Experiments were conducted in triplicate.

Quantitative real-time PCR

Total RNA was extracted from cells using an Omega R6934-01 Total RNA Kit (Omega Bio-tek, Norcross, GA, USA) according to the manufacturer's protocol. cDNA synthesis was performed using PrimeScript RT Reagent (DRR037A; Takara Bio, Shiga, Japan) following the manufacturer's instructions. qPCR was performed on a Q3 LightCycler 2.0 instrument using

SYBR Premix Ex Taq (DRR081A; Takara Bio), and results were calculated using the $2^{-\Delta\Delta C_t}$ method [27]. The *MMP-1*, *MMP-2*, *MMP-9*, and *GAPDH* primers were synthesized by Shanghai Sangon Co (Shanghai, China) as described previously [28], and the *LGALS3* and *MGAT5* primers were synthesized by Beijing Genomics Institute (BGI, Shenzhen, China).

Immunoprecipitation, western blotting, and lectin blotting

Cells were harvested in lysis buffer and total protein concentrations were determined using a BCA Protein Assay Kit (Thermo Fisher Scientific, Waltham, MA, USA). Immunoprecipitation (IP) was performed using a Thermo Scientific Pierce co-IP and cross-linking kit according to the manufacturer's protocol. Briefly, after immobilizing the antibody for 3 h, the resin and lysate were incubated at 4 °C overnight. Afterwards, the proteins were eluted and analyzed by western blotting. An IgG antibody was immobilized as a negative control to assess nonspecific binding.

Proteins were separated by 10% SDS-PAGE and transferred to PVDF membranes (Millipore, Billerica, MA, USA). After the membranes were blocked with 5% fat-free milk, they were incubated with the indicated primary antibody at 4 °C overnight. The levels of β 1,6-GlcNAc-branched *N*-glycans were detected by lectin blotting. After blocking with 3% BSA in TBS (Tris-buffered saline; 20 mM Tris and 0.5 M NaCl, pH 7.5), blots were incubated overnight with biotinylated PHA-L (1:1000 dilution) [22]. After washing with PBST, the membranes were incubated with avidin-HRP (1:1000 dilution) for 1 h and then washed with PBST. Staining was detected with ECL western blotting detection reagents.

Fluorescence-activated cell sorting (FACS)

Briefly, cells were harvested, washed twice with PBS, stained with fluorescein-labeled PHA-L (1:500) for 0.5 h on ice in the dark, and then washed twice [29]. The cells were analyzed by flow cytometry using FlowJo 7.6 software.

Statistical analysis

Statistical analyses were performed using SPSS or GraphPad Prism 5. All data were analyzed by two-tailed *t*-tests or analysis of variance (ANOVA) as appropriate, and $p < 0.05$ was considered statistically significant.

Results

Upregulation of β 1,6-GlcNAc glycans on CD147/basigin in hepatocytes during TGF- β 1-induced EMT

EMT facilitates tumor metastasis and has recently been identified as a crucial driver of tumor progression [30,31]. In our research, a correlation between

GnT-V expression and EMT was observed in the cell lines tested. GnT-V-mediated glycosylation was elevated in QZG cells when EMT was induced by 24-h treatment with 2.5 ng/ml TGF- β 1 (Figure 1A–D). As shown in Figure 1E, F, CD147/basigin was upregulated in QZG cells during TGF- β 1-induced EMT. To further determine whether CD147/basigin glycosylation is associated with EMT, we analyzed the ratio of glycosylated/non-glycosylated protein by western blotting. The increase in this ratio suggested the upregulation of CD147/basigin *N*-glycosylation (Figure 1G). Next, we detected the levels of β 1,6-GlcNAc glycans using PLA and IP with lectin blotting after TGF- β 1-induced EMT. We observed an increase in CD147/basigin- β 1,6-branching after TGF- β 1 treatment (Figure 1H–J).

CD147/basigin- β 1,6-branching in HCC correlates with tumor metastasis

We evaluated the clinical relevance of CD147/basigin- β 1,6-branching levels in HCC patients. CD147/basigin is detected in both tumor and adjacent tissue (Figure 2A). While our previous research found that CD147/basigin from human lung cancer tissue contains a high percentage of core fucose and β 1,6-GlcNAc glycans, the constitution of CD147/basigin glycosylation in HCC remained unclear [22]. Lectin histochemistry (Figure 2A) of 14 HCC patient samples showed marked positive reactivity of biotinylated PHA-L, demonstrating a high level of β 1,6-GlcNAc-branched *N*-glycans, whereas either negative or weak LCA signals were observed, confirming that core fucosylation is not universal in HCC tissue, as previously reported [9]. Because adjacent HCC tissues were positive for both PHA-L and LCA, we next investigated β 1,6-glycans as a target. As the levels of CD147/basigin glycosylation in HCC were unknown, we assessed the levels of β 1,6-branched glycans in HCC tissue and cancer cell lines (Figure 2B and supplementary material, Figure S1) and found high levels on the plasma membrane. Furthermore, our PLA results (Figure 2B) confirmed that CD147/basigin was highly glycosylated with β 1,6-branching in HCC, which is consistent with previous findings [32,33]. To determine the correlation with prognostic features in HCC, 51 patients with HCC were analyzed; only Barcelona clinic liver cancer (BCLC) stage was related to the level of CD147/basigin- β 1,6-branched glycans (Table 1, $p = 0.016$). Next, we further analyzed the correlation between BCLC stage and CD147/basigin- β 1,6-branched glycans. Tissues from patients with stage C disease were markedly positive for CD147/basigin- β 1,6-branched *N*-glycans (PLA signal), whereas only weak signals were observed in tissues from patients with stage 0–A disease ($p = 0.002$, Figure 2C, D); this modification increased as the staging progressed (Figure 2D). These results indicate that the level of CD147/basigin- β 1,6-branched glycans is linked to HCC metastasis and progression.

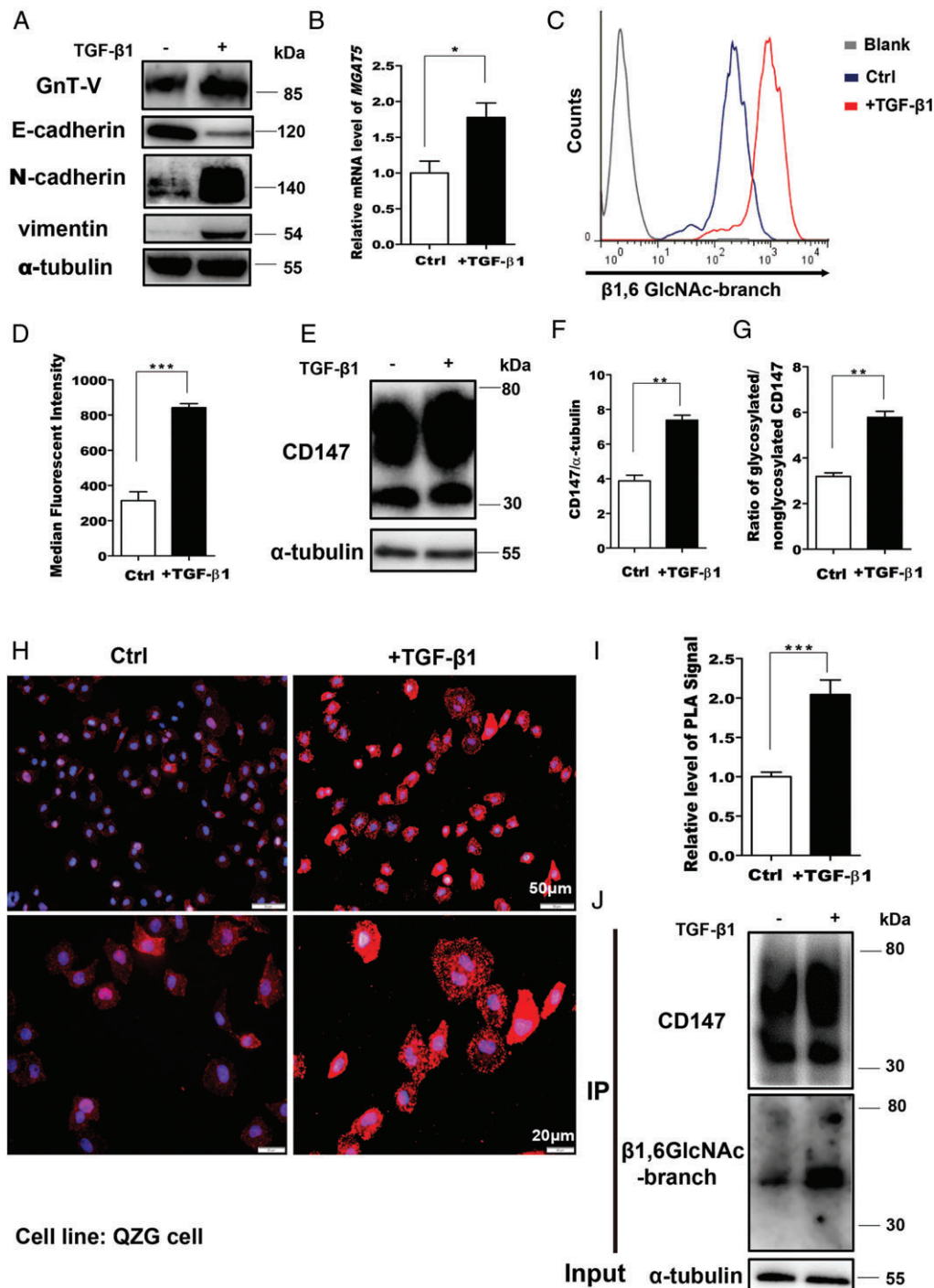


Figure 1. The level of CD147-β1,6-GlcNAc-branched structures is enhanced during EMT. (A) Cells were treated with 2.5 ng/ml TGF-β1 for 24 h and cell lysates were analyzed by western blotting. (B) Real-time PCR detection of *MGAT5* mRNA levels in QZG cells stimulated with 2.5 ng/ml TGF-β1 for 24 h. *GAPDH* was used as the normalization control. (C, D) Membrane levels of β1,6-GlcNAc branching were measured by FACS with fluorescein-labeled PHA-L in QZG cells stimulated with TGF-β1 for 24 h. (E–G) Western blotting of CD147, CD147/tubulin, and glycosylated/non-glycosylated CD147 in control and TGF-β1-treated cells. (H, I) *In situ* PLA in control cells and cells treated with TGF-β1. (H) Representative image. (I) Quantification. (J) QZG cells treated with TGF-β1 were subjected to CD147/HAB18G immunoprecipitation (IP), western blotting, and lectin analyses. The results are shown as the mean ± SD ($n=3$). Significance was determined by Student's *t*-test (* $p < 0.05$; ** $p < 0.01$; *** $p < 0.001$).

GnT-V-mediated glycosylation promotes CD147/basigin-mediated invasion in HCC cells

We next assessed the effect of GnT-V-mediated glycosylation of CD147/basigin on the invasive properties of HCC cells. Inhibition of β1,6-branching synthesis

using 1 μg/ml swainsonine (supplementary material, Figure S2) or attenuation of *MGAT5* expression with siRNA (si-*MGAT5*) markedly reduced cell invasion and migration (Figure 3A, B). To determine the effect of β1,6-branched *N*-glycosylation, we stimulated Huh-7 and HepG2 cells with purified wild-type or with

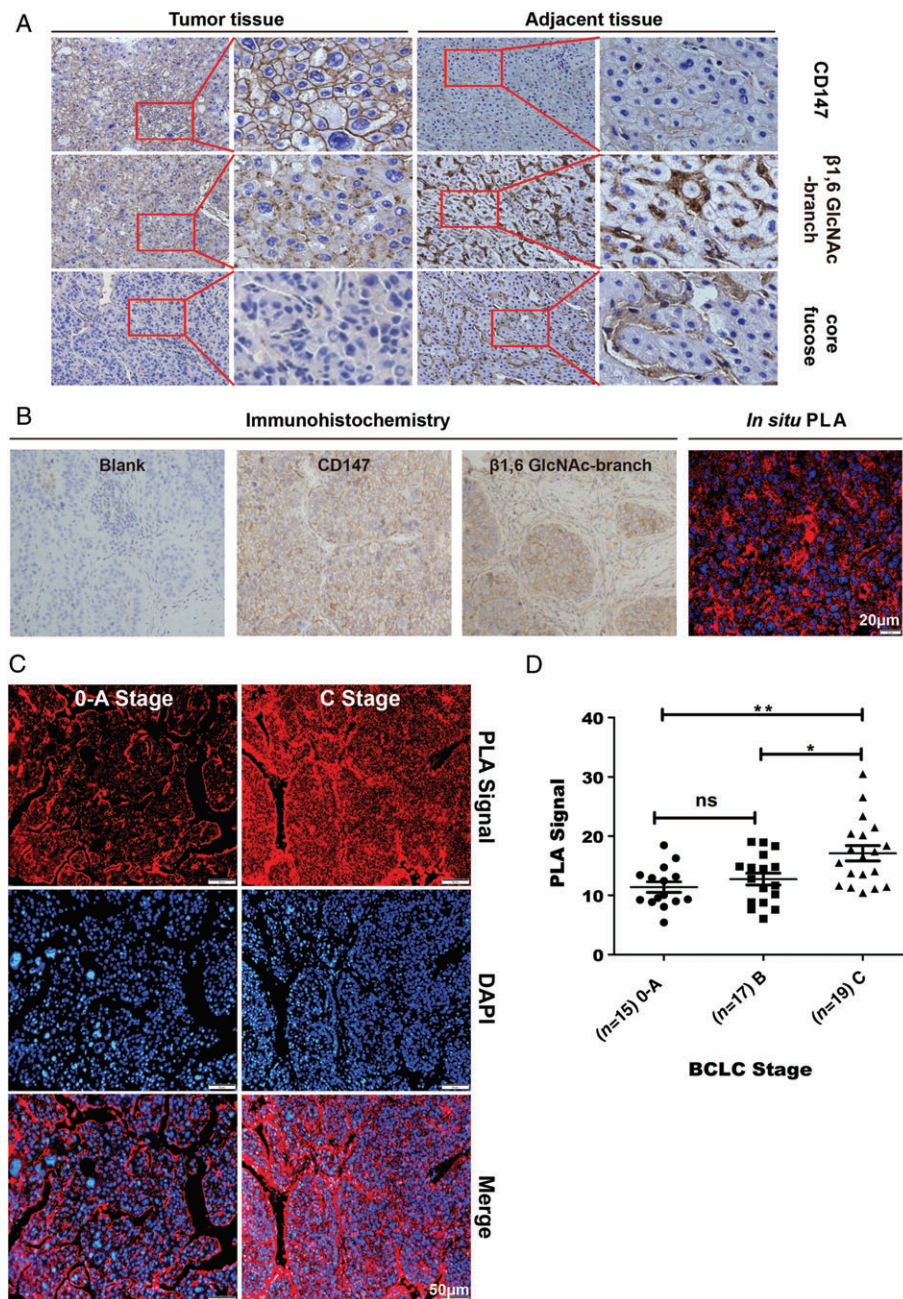


Figure 2. Evaluation of CD147 and β 1,6-GlcNAc-branched structures in human HCC tissues in different BCLC stages ($n=51$). (A) Immunohistochemistry of HAB18G/CD147, β 1,6-GlcNAc-branched *N*-glycans, and core fucose in HCC tumor tissues and adjacent tissues ($400\times$, $n=14$). In total, 14/14 tumor tissues had positive signals for PHA-L and β 1,6-GlcNAc-branched structures, while 1/14 expressed core fucose. All adjacent tissues expressed both β 1,6-GlcNAc-branched *N*-glycans and core fucose. (B) Immunohistochemistry of HAB18G/CD147 and β 1,6-GlcNAc-branched *N*-glycans and PLA assay of CD147- β 1,6-GlcNAc branching in the same tumor tissues ($400\times$). Scale bar = 20 μ m. (C) *In situ* PLA detecting CD147 with β 1,6-GlcNAc-branched structures in human HCC tissue stage 0–A and stage C HCC tissue. Scale bar = 50 μ m. (D) Quantitation of PLA signals. $p=0.002$ (stage C versus 0–A); $p=0.018$ (stage C versus B); $p=0.685$ (stage B versus 0–A). * $p<0.05$; ** $p<0.01$; one-way ANOVA.

mutant CD147/basigin with defective β 1,6-branched *N*-glycosylation, and then analyzed MMP expression (Figure 3C, D). Real-time PCR showed that *MMP-1*, *MMP-2*, and *MMP-9* were reduced in cells treated with mutant CD147/basigin (defective β 1,6-branched *N*-glycosylation) compared with cells treated with wild-type, suggesting that GnT-V-mediated glycosylation increases CD147/basigin-mediated HCC cell invasion (Figure 3D).

β 1,6-GlcNAc glycans are required for the interaction between CD147/basigin and integrin β 1

Integrin β 1 is one of the most predominant interacting partners of CD147/basigin [18]. To assess the contribution of *N*-glycosylation to the interaction with integrin β 1, we constructed WT-CD147-GFP and 3Q-CD147-GFP plasmids (Figure 4A). After transfection into HEK293T cells, a strong green fluorescence

Table 1. Correlation between aberrant glycosylation of CD147/basigin mediated by GnT-V and prognostic variables in 51 HCC patients. Statistical significance of differences between groups was analyzed by the Wilcoxon rank sum test

Variable	PLA signal CD147/PHA-L	
	Median (minimum–maximum)	<i>P</i> value
Sex		0.375
Male (<i>n</i> = 38)	13.48 (5.41–30.48)	
Female (<i>n</i> = 11)	11.43 (8.07–18.37)	
Age (years)		0.829
<50 (<i>n</i> = 22)	11.63 (5.41–30.80)	
≥50 (<i>n</i> = 15)	12.8 (6.04–20.40)	
Liver cirrhosis		0.335
Yes (<i>n</i> = 30)	13.64 (5.41–30.48)	
No (<i>n</i> = 19)	11.43 (7.59–20.40)	
BCLC stage		0.016
0–A (<i>n</i> = 15)	10.05 (5.41–17.65)	
B–C (<i>n</i> = 36)	14.60 (6.04–30.48)	
PVT		0.242
Yes (<i>n</i> = 9)	13.54 (10.42–20.40)	
No (<i>n</i> = 26)	12.00 (6.04–26.54)	
Number of tumors		0.133
< 3 (<i>n</i> = 44)	12.63 (5.41–30.48)	
> 3 (<i>n</i> = 5)	15.49 (13.54–18.37)	
Tumor size (cm)		0.080
≤ 5 (<i>n</i> = 19)	12.46 (5.41–18.45)	
> 5 (<i>n</i> = 31)	14.28 (6.04–30.48)	
Serum AFP (μg/l)		0.178
≤ 25 (<i>n</i> = 10)	12.06 (7.59–18.32)	
> 25 (<i>n</i> = 38)	13.80 (5.41–30.48)	

PHA-L = biotinylated *Phaseolus vulgaris* leucoagglutinin; PLA = proximity ligation assay.

signal was observed by fluorescence microscopy (supplementary material, Figure S3). When integrin β1 was immunoprecipitated from cell lysates, the precipitated GFP levels were much lower in 3Q-293 T cells than in WT-293 T cells (Figure 4B). The reverse was also true, suggesting that 3Q-CD147 is less efficient at binding integrin β1 than WT-CD147, and indicating that the binding of CD147/basigin to integrin β1 is affected by *N*-glycosylation. We next analyzed the interaction of integrin β1 and CD147/basigin by PLA. When β1,6-GlcNAc glycan synthesis was inhibited for 48 h by swainsonine or si-*MGAT5* (Figure 4C–F), there was a decrease in the ability of CD147/basigin to bind integrin β1. β1,6-GlcNAc glycans are the preferred binding partners of galectin-3, an *N*-glycan-binding ligand, in the formation of functional extracellular galectin glycoprotein lattices [34]. To further confirm the role of β1,6-GlcNAc glycans in this interaction, we silenced *LGALS3* gene expression using siRNA. As determined by co-IP and western blotting, si-*LGALS3* reduced the interaction between CD147/basigin and integrin β1 compared with control (Figure 4G, H). These findings clearly establish the importance of β1,6-GlcNAc glycans for the binding of CD147/basigin to integrin β1, consistent with the previous result that CD147/basigin-β1,6-branched glycans are associated with metastasis.

The PI3K/Akt signaling pathway is involved in the regulation of GnT-V expression

CD147/basigin interacts with integrin β1 and activates the PI3K/Akt pathway. To investigate whether GnT-V is linked to the PI3K pathway, we treated HepG2 and Huh-7 cells with 10 μmol/l LY294002, a PI3K inhibitor [36]. Western blotting and qPCR showed that GnT-V and Gal-3 were decreased by LY294002 (Figure 5A–C). As shown in Figure 4, β1,6-GlcNAc glycans regulated the CD147/basigin–integrin β1 interaction. To determine whether they also regulate the downstream PI3K pathway, we analyzed activation of downstream proteins, including FAK, paxillin, and Akt. Depletion of β1,6-branched *N*-glycans impaired PI3K pathway activation and the subsequent activation of p-FAK, p-paxillin, and p-Akt (Figure 5D); these results were comparable to those of previous studies [36,37]. Taken together, activation of the PI3K/Akt pathway is involved in the regulation of GnT-V expression and deletion of GnT-V-mediated *N*-glycosylation impairs the PI3K/Akt pathway.

Discussion

In the current study, we determined how β1,6-branched *N*-glycans contribute to the biological functions of CD147/basigin in HCC metastasis. EMT is an important process for metastasis [38] and emerging evidence suggests a correlation between GnT-V and EMT. The expression of GnT-V is elevated during EMT [39,40] and GnT-V overexpression promotes TGF-β-induced EMT and enhances the metastasis of multiple types of carcinoma [41,42]. However, some inconsistent results have also been reported; for example, GnT-V was reported to suppress EMT in lung cancer cells [43]. Our research showed that GnT-V was upregulated during TGF-β1-induced EMT in hepatocytes. In our previous study, we characterized the role of CD147/basigin in promoting EMT in HCC progression at the transcriptional level, and we thus wondered whether GnT-V-mediated *N*-glycosylation of CD147/basigin changes during EMT. Analysis of CD147/basigin-β1,6-branching confirmed that modifications were increased, implying that β1,6-branched glycans are involved in the functions of CD147/basigin in metastasis.

We confirmed this finding in patients with HCC by quantifying the levels of CD147/basigin-β1,6-branched glycans in HCC tissues *in situ*. The positive correlation between the level of branched CD147/basigin-β1,6-glycans and BCLC stage indicates that CD147/basigin-β1,6-branching is correlated with HCC metastasis. As mentioned previously, CD147/basigin was initially identified as an inducer of MMPs (termed EMMPRIN; extracellular matrix metalloproteinase inducer) and MMPs are often increased in cancer in correlation with tumor invasiveness and

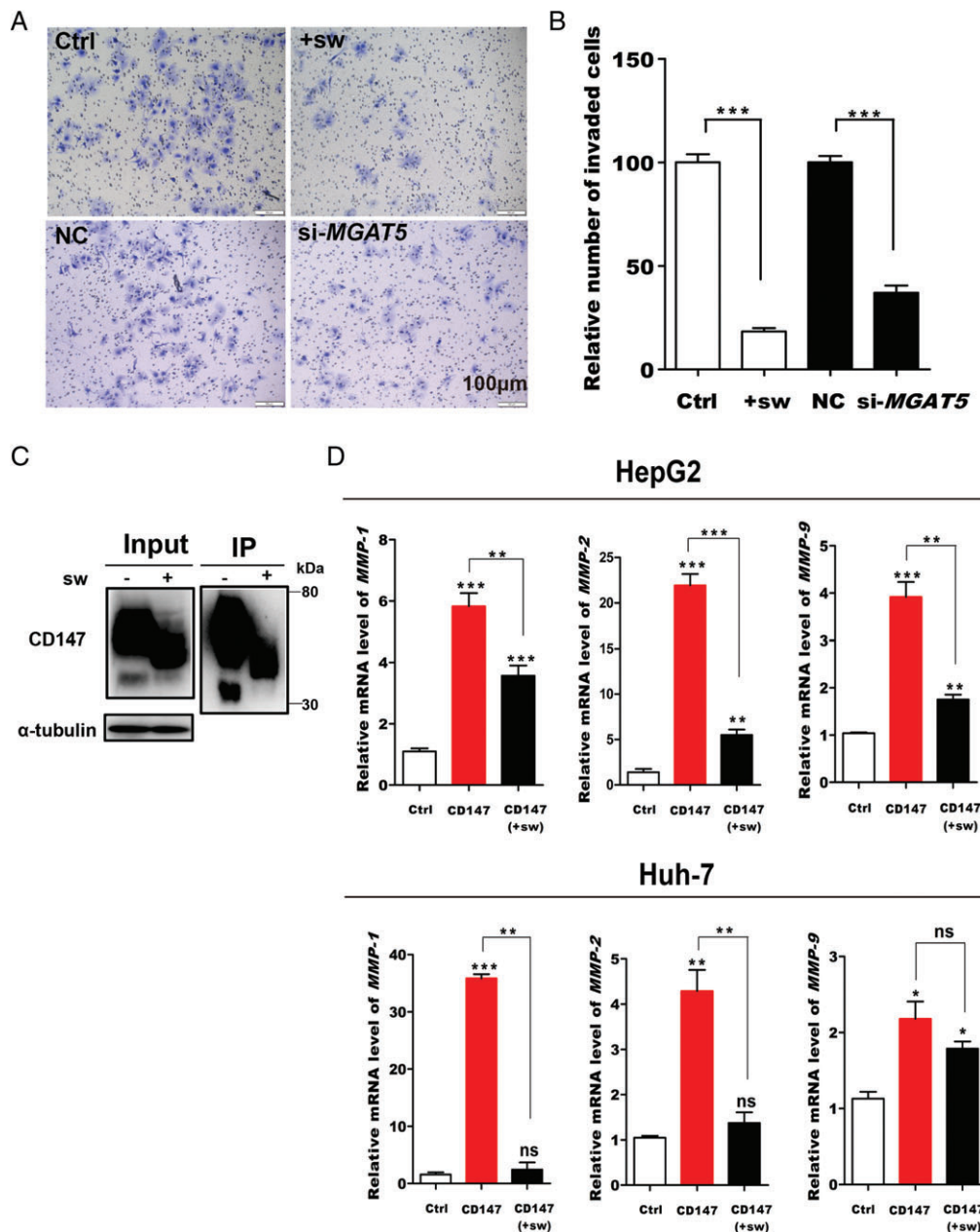


Figure 3. β 1,6-GlcNAc-branched structures on CD147 promote invasion and metastasis in HCC cells. (A, B) Invasive potential of Huh-7 cells. (A) Representative images. (B) Quantification of +sw (treatment with 1 μ g/ml swainsonine for 48 h) and the effect of *MGAT5* silencing. (C) Huh-7 and HepG2 cells treated with 1 μ g/ml swainsonine (sw) for 48 h were subjected to CD147/HAb18G immunoprecipitation and western blotting. (D) Actively growing HepG2 and Huh-7 cells were treated with purified CD147 protein (1 μ g/ml) for 24 h. The mRNA levels of *MMP-1*, *MMP-2*, and *MMP-9* in HepG2 and Huh-7 cells were quantitated by real-time PCR. Data are presented as the mean \pm SD of three independent experiments. * $p < 0.05$; ** $p < 0.01$; *** $p < 0.001$.

metastasis. Inhibiting the addition of β 1,6-branched glycans onto CD147/basigin with swainsonine decreased MMP expression in HepG2 and Huh-7 cells. In contrast, overexpression of GnT-V increased the level of CD147/basigin- β 1,6-branching and the induction of MMPs [22]. These results suggest that the GnT-V-mediated *N*-glycosylation of CD147/basigin increases its biological activity in metastasis.

N-glycosylation plays a role in protein–protein interactions [44–46]. CD147/basigin interacts with integrin β 1 to modulate integrin-dependent signaling and FAK activation, leading to downstream events such

as stimulation of the Rac/Ras/Raf/ERK and PI3K/Akt pathways, and enhancing the invasive and metastatic potential of HCC cells [47]. Although the effects of *N*-glycosylation on integrin β 1 binding to other proteins have been partially revealed, the fundamental mechanism by which glycans affect this interaction is not well understood [46,48]. We explored whether β 1,6-branched glycans play a role in the interaction between CD147/basigin and integrin β 1. PLA showed that the binding of CD147/basigin to integrin β 1 was decreased when β 1,6-branched glycan synthesis was inhibited or when *MGAT5* expression was silenced, and

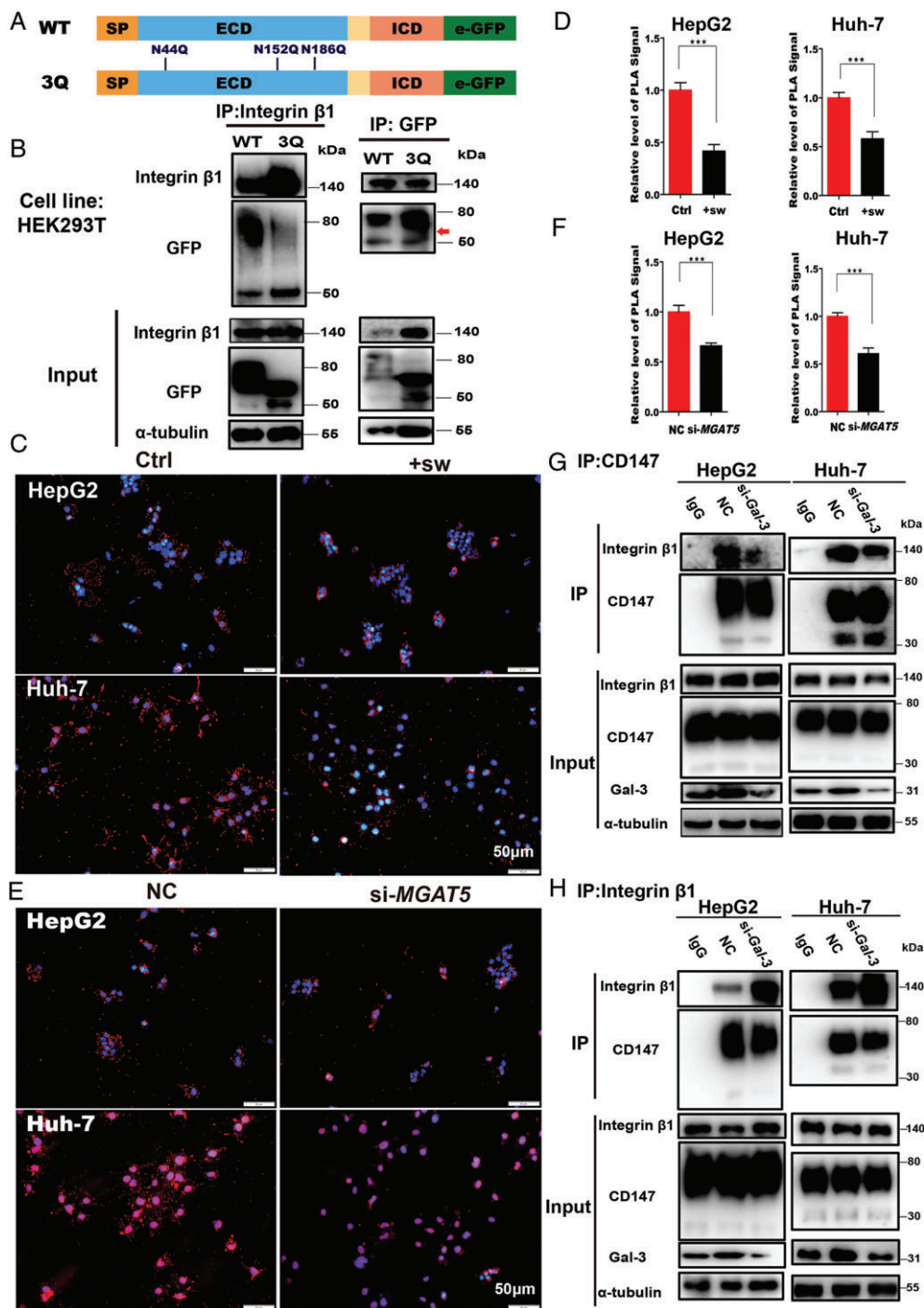


Figure 4. CD147/basigin-β1,6-GlcNAc branching is required for the interaction with integrin β1. (A) Schematic diagram of the CD147/basigin protein. Full-length protein was separated into the extracellular domain (ECD) and the intracellular domain (ICD). SP = signal peptide; TM = transmembrane domain. Three *N*-glycosylation sites in the ECD domain are labeled in blue (numbers indicate amino acid position). (B) Co-IP of HEK293T cells transfected with WT-CD147-GFP or 3Q-CD147-GFP plasmid. Left: CD147-GFP was immunoprecipitated with anti-integrin β1 and detected using anti-GFP (upper panel); 1/10th of the total cell lysate was analyzed as input protein (lower panel). Right: integrin β1 was immunoprecipitated with GFP and CD147-GFP was detected using anti-GFP antibodies (upper panel; red arrow indicates a higher level of heavily glycosylated 3Q-CD147); 1/10th of the total cell lysate was analyzed as input protein (lower panel). (C, D) Fluorescence signal and *in situ* PLA analysis of the interaction between CD147 and integrin β1 under the indicated conditions (sw, 1 μg/ml). Scale bar = 50 μm. (E, F) Fluorescence signal and *in situ* PLA analysis of the interaction between CD147 and integrin β1 after silencing *MGAT5*. Scale bar = 50 μm. (G, H) Co-IP of CD147 and integrin β1 in HepG2 and Huh-7 cells transfected with either siRNAs targeting *LGALS3* (*Gal-3*) or nonspecific control (NC) siRNA. (G) Immunoprecipitation with HA18G/CD147 antibodies (upper panel); input proteins were detected (lower panel). (H) Immunoprecipitation with integrin β1 antibodies (upper panel); input proteins were detected (lower panel). In G and H, the input represents 1/10th of the total cell lysate (comprising si-*Gal-3* and NC samples mixed with IgG). All data are presented as the mean ± SD of three independent experiments. **p* < 0.05; ***p* < 0.01; ****p* < 0.001.

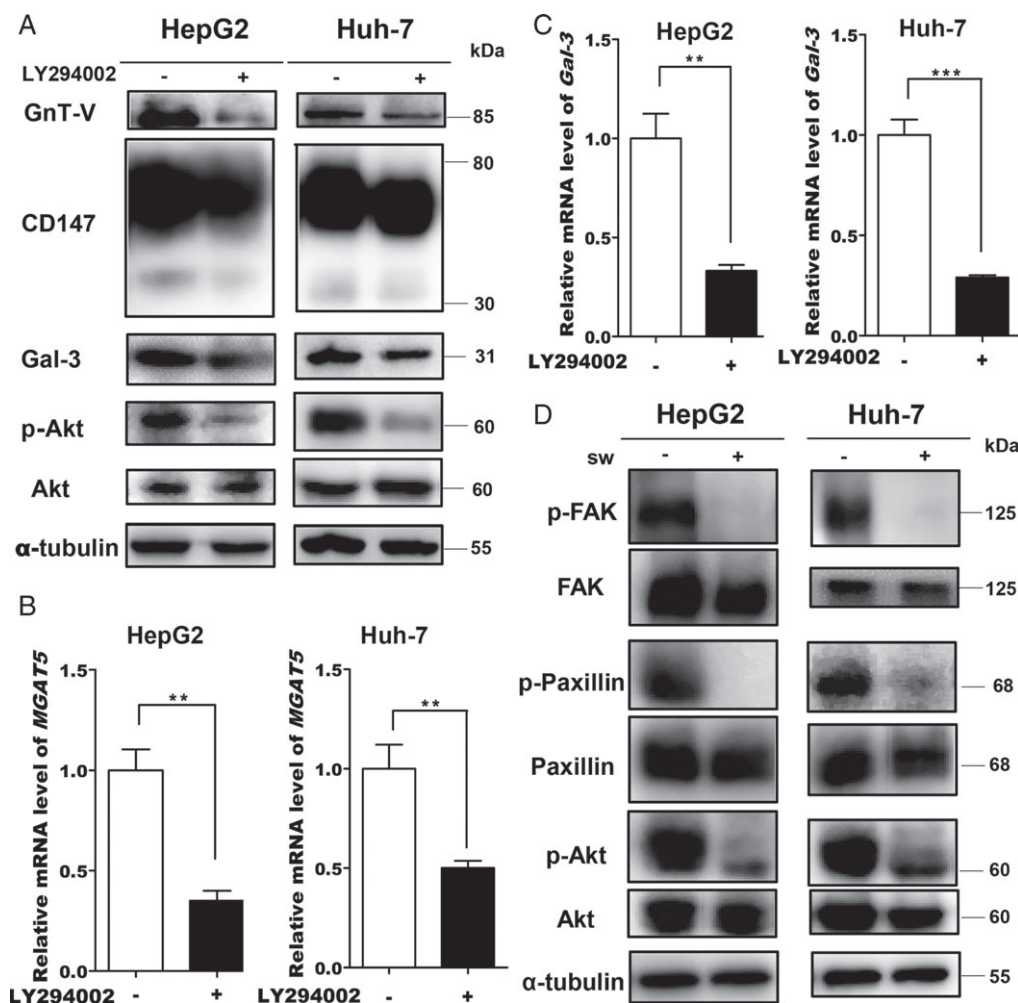


Figure 5. The PI3K/Akt signaling pathway is involved in the regulation of GnT-V expression. (A, B) GnT-V in cells treated with 10 $\mu\text{mol/l}$ LY294002 for 24 h. (A) Western blotting. (B) Real-time PCR. (C) Real-time PCR analysis of *LGALS3* (*Gal-3*) in cells treated with 10 $\mu\text{mol/l}$ LY294002 for 24 h. (D) Western blotting of PI3K-dependent signaling under the indicated conditions (sw, 1 $\mu\text{g/ml}$). All data are presented as the mean \pm SD ($n = 3$). * $p < 0.05$; ** $p < 0.01$; *** $p < 0.001$.

silencing *LGALS3* had a similar effect. These results reveal that β 1,6-branched glycans play a crucial role in the interaction between CD147/basigin and integrin β 1. However, inhibiting *N*-glycosylation of CD147/basigin did not fully abrogate the interaction (Figure 4B), suggesting that other factors are involved, as previously reported [47]. In addition, β 1,6-branched glycans might act as co-receptors to promote the interaction between CD147/basigin and integrin β 1. Based on these results, we conclude that β 1,6-glycans modulate CD147/basigin-mediated functions in metastasis.

Accumulating evidence suggests that activated FAK–paxillin and FAK–PI3K signaling pathways are actively engaged in the migratory process in metastatic cancer cells [49]. Our laboratory previously discovered that PI3K signaling enhances the metastatic potential of HCC cells, which is closely correlated with CD147/basigin expression [15,50]. While *MGAT5* expression is reportedly regulated by the RAS–RAF–MAPK signaling pathway [8], the regulatory effect of the PI3K pathway on *MGAT5* has not yet been revealed. The current study showed

that the PI3K/Akt pathway regulates GnT-V expression and the *N*-glycosylation of CD147/basigin. CD147/basigin interacts with integrin β 1 and activates the downstream FAK–PI3K pathway, and inhibition of β 1,6-glycans decreased this interaction. Thus, inhibition of β 1,6-glycans would theoretically attenuate the PI3K pathway, and we verified this phenomenon in Huh-7 and HepG2 cells. Interruption of β 1,6-branched glycans by swainsonine suppressed the PI3K/Akt pathway, and these results were comparable to those reported by Guo *et al* [37]. Moreover, the PI3K pathway regulates EMT [51]. The levels of GnT-V and CD147/basigin- β 1,6-branched glycans were upregulated during EMT, which enhanced the interaction with integrin β 1 (Figure 4), further promoting PI3K/Akt pathway activation [15] and enhancing the invasive and metastatic potential of HCC cells. However, it should be noted that GnT-V mediates the glycosylation of not only CD147/basigin but also all proteins that contain β 1,6-branching. Using CD147/basigin as a model, our data suggest that β 1,6-branching affects the affinity and biological functions of many other glycoproteins.

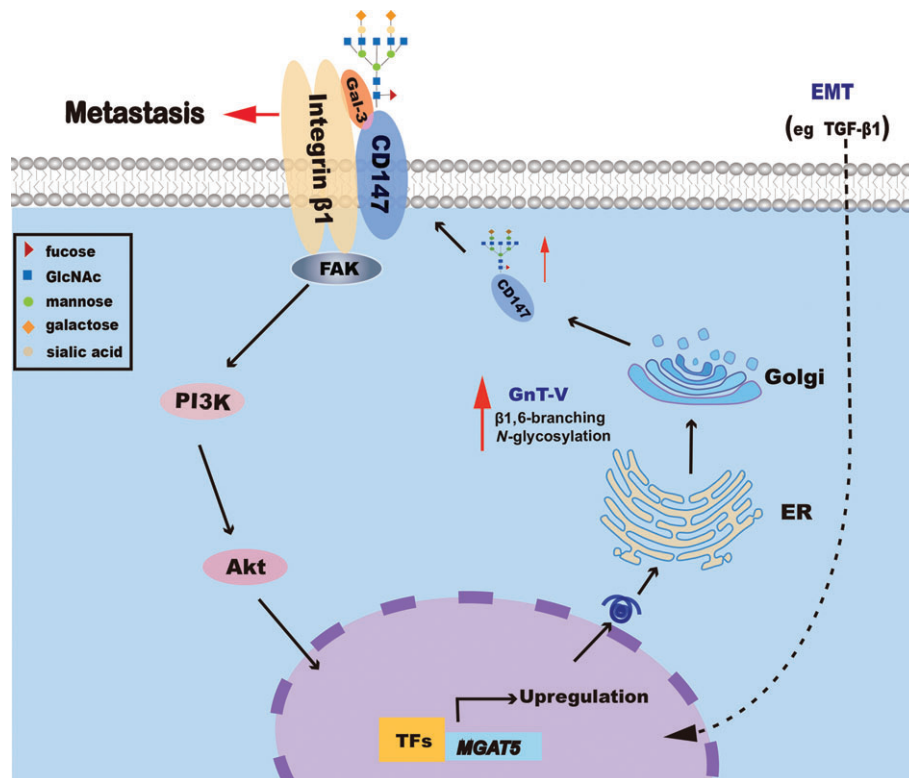


Figure 6. Proposed positive feedback loop for the regulation of PI3K/Akt and GnT-V to promote HCC metastasis. During EMT, transcription factors (TFs) accumulate in the nuclei of cancer cells to activate GnT-V expression. GnT-V then leads to global alteration of β 1,6-branched glycans on cell surface molecules, including CD147/basigin, altering the response of cancer cells to their microenvironment, which consequently promotes metastasis. When the PI3K/Akt pathway is inhibited, GnT-V expression decreases; furthermore, PI3K signaling is suppressed when the synthesis of β 1,6-GlcNAc-branched *N*-glycans catalyzed by GnT-V is interrupted.

Based on the findings of this study, we propose a model to explain the molecular mechanism of GnT-V in HCC progression (Figure 6). During EMT, transcription factors accumulate in the nuclei of cancer cells to activate GnT-V expression. The modification of surface molecules such as CD147/basigin with β 1,6-branched glycans is increased, which alters the response of cancer cells to their microenvironment. These alterations lead to changes in cell behavior, facilitating metastasis. In addition, β 1,6-GlcNAc-branched *N*-glycans regulate the interaction of CD147/basigin with integrin β 1 and the associated downstream signaling events. Moreover, the PI3K/Akt signaling pathway regulates GnT-V expression, and the products of this enzyme affect PI3K/Akt signaling.

In conclusion, we have demonstrated a novel mechanism by which β 1,6-branched *N*-glycans regulate the activity of CD147/basigin in the metastasis of HCC cells, and these modifications are critical for EMT and the interaction with integrin β 1. In addition, we propose a feedback model in which the PI3K/Akt pathway regulates GnT-V expression, and this enzyme then enhances the PI3K signal. Our study not only reveals the pathological role and regulatory mechanism of GnT-V-mediated modification of CD147/basigin during HCC progression but also sheds light on promising prognostic factors and personalized therapeutic leads to target HCC and possibly other cancers.

Acknowledgements

This work was supported by grants from the National Basic Research Program of China (2015CB553701) and the National Natural Science Foundation of China (81402383, 31601127).

Author contributions statement

JC, WH, and J-LJ conceived the research. LL, J-LJ, JJ, JL, W-PS, Z-YL, and JC designed the methodology. JC performed the experiments. JC, WH, and BW wrote the original draft of the manuscript. J-LJ and Z-NC reviewed and edited the manuscript. WH, J-LJ, and Z-NC were involved in acquiring funding. JC, WH, BW, LY, and DL were involved in obtaining resources. Z-NC and J-LJ supervised the study. All authors gave final approval of the submitted and published versions of the manuscript.

References

1. Stowell SR, Ju T, Cummings RD. Protein glycosylation in cancer. *Annu Rev Pathol* 2015; **10**: 473–510.
2. Reticker-Flynn NE, Bhatia SN. Aberrant glycosylation promotes lung cancer metastasis through adhesion to galectins in the metastatic niche. *Cancer Discov* 2015; **5**: 168–181.

3. Magalhães A, Duarte HO, Reis CA. Aberrant glycosylation in cancer: a novel molecular mechanism controlling metastasis. *Cancer Cell* 2017; **31**: 733–735.
4. Cheng C, Ru P, Geng F, *et al*. Glucose-mediated N-glycosylation of SCAP is essential for SREBP-1 activation and tumor growth. *Cancer Cell* 2015; **28**: 569–581.
5. Wojtowicz K, Januchowski R, Nowicki M, *et al*. Inhibition of protein glycosylation reverses the MDR phenotype of cancer cell lines. *Biomed Pharmacother* 2015; **74**: 49–56.
6. Glavey SV, Huynh D, Reagan MR, *et al*. The cancer glycome: carbohydrates as mediators of metastasis. *Blood Rev* 2015; **29**: 269–279.
7. Pinho SS, Reis CA. Glycosylation in cancer: mechanisms and clinical implications. *Nat Rev Cancer* 2015; **15**: 540–555.
8. Dennis JW, Laferte S, Waghorne C, *et al*. Beta 1-6 branching of Asn-linked oligosaccharides is directly associated with metastasis. *Science* 1987; **236**: 582–585.
9. Taniguchi N, Kizuka Y. Glycans and cancer: role of N-glycans in cancer biomarker, progression and metastasis, and therapeutics. *Adv Cancer Res* 2015; **126**: 11–51.
10. Sato Y, Nakata K, Kato Y, *et al*. Early recognition of hepatocellular carcinoma based on altered profiles of alpha-fetoprotein. *N Engl J Med* 1993; **328**: 1802–1806.
11. Grass GD, Dai L, Qin Z, *et al*. CD147: regulator of hyaluronan signaling in invasiveness and chemoresistance. *Adv Cancer Res* 2014; **123**: 351–373.
12. Li Y, Xu J, Chen L, *et al*. HAb18G (CD147), a cancer-associated biomarker and its role in cancer detection. *Histopathology* 2009; **54**: 677–687.
13. Muramatsu T. Basigin (CD147), a multifunctional transmembrane glycoprotein with various binding partners. *J Biochem* 2016; **159**: 481–490.
14. Sidhu SS, Nawroth R, Retz M, *et al*. EMMPRIN regulates the canonical Wnt/ β -catenin signaling pathway, a potential role in accelerating lung tumorigenesis. *Oncogene* 2010; **29**: 4145–4156.
15. Wu J, Ru N, Zhang Y, *et al*. HAb18G/CD147 promotes epithelial–mesenchymal transition through TGF- β signaling and is transcriptionally regulated by Slug. *Oncogene* 2011; **30**: 4410–4427.
16. Zhao P, Zhang W, Wang S, *et al*. HAb18G/CD147 promotes cell motility by regulating annexin II-activated RhoA and Rac1 signaling pathways in hepatocellular carcinoma cells. *Hepatology* 2011; **54**: 2012–2024.
17. Tang J, Guo Y, Zhang Y, *et al*. CD147 induces UPR to inhibit apoptosis and chemosensitivity by increasing the transcription of Bip in hepatocellular carcinoma. *Cell Death Differ* 2012; **19**: 1779–1790.
18. Wu J, Li Y, Dang YZ, *et al*. HAb18G/CD147 promotes radioresistance in hepatocellular carcinoma cells: a potential role for integrin β 1 signaling. *Mol Cancer Ther* 2015; **14**: 553–563.
19. Wu B, Liu ZY, Cui J, *et al*. F-box protein FBXO22 mediates polyubiquitination and degradation of CD147 to reverse cisplatin resistance of tumor cells. *Int J Mol Sci* 2017; **18**: 212.
20. Yu X, Jiang J, Li L, *et al*. The glycosylation characteristic of hepatoma-associated antigen HAb18G/CD147 in human hepatoma cells. *Int J Biochem Cell B* 2006; **38**: 1939–1945.
21. Bai Y, Huang W, Ma L, *et al*. Importance of N-glycosylation on CD147 for its biological functions. *Int J Mol Sci* 2014; **15**: 6356–6377.
22. Huang W, Luo W, Zhu P, *et al*. Modulation of CD147-induced matrix metalloproteinase activity: role of CD147 N-glycosylation. *Biochem J* 2013; **449**: 437–448.
23. Tang W. Links between CD147 function, glycosylation, and caveolin-1. *Mol Biol Cell* 2004; **15**: 4043–4050.
24. Li J, Huang W, Lin P, *et al*. N-linked glycosylation at Asn152 on CD147 affects protein folding and stability: promoting tumour metastasis in hepatocellular carcinoma. *Sci Rep* 2016; **6**: 35210.
25. Jia L, Zhou H, Wang S, *et al*. Deglycosylation of CD147 down-regulates matrix metalloproteinase-11 expression and the adhesive capability of murine hepatocarcinoma cell HcaF *in vitro*. *IUBMB Life* 2006; **58**: 209–216.
26. Ku XM, Liao CG, Li Y, *et al*. Epitope mapping of series of monoclonal antibodies against the hepatocellular carcinoma-associated antigen HAb18G/CD147. *Scand J Immunol* 2007; **65**: 435–443.
27. Livak KJ, Schmittgen TD. Analysis of relative gene expression data using real-time quantitative PCR and the $2^{-\Delta\Delta CT}$ method. *Methods* 2001; **25**: 402–408.
28. Fu ZG, Wang L, Cui HY, *et al*. A novel small-molecule compound targeting CD147 inhibits the motility and invasion of hepatocellular carcinoma cells. *Oncotarget* 2016; **7**: 9429–9447.
29. Wu B, Cui J, Yang X, *et al*. Cytoplasmic fragment of CD147 generated by regulated intramembrane proteolysis contributes to HCC by promoting autophagy. *Cell Death Dis* 2017; **8**: e2925.
30. Nieto MA, Huang RY, Jackson RA, *et al*. EMT: 2016. *Cell* 2016; **166**: 21–45.
31. Lambert AW, Pattabiraman DR, Weinberg RA. Emerging biological principles of metastasis. *Cell* 2017; **168**: 670–691.
32. Carvalho S, Catarino TA, Dias AM, *et al*. Preventing E-cadherin aberrant N-glycosylation at Asn-554 improves its critical function in gastric cancer. *Oncogene* 2016; **35**: 1619–1631.
33. Caldieri G, Barbieri E, Nappo G, *et al*. Reticulon 3-dependent ER–PM contact sites control EGFR nonclathrin endocytosis. *Science* 2017; **356**: 617–624.
34. Lakshminarayan R, Wunder C, Becken U, *et al*. Galectin-3 drives glycosphingolipid-dependent biogenesis of clathrin-independent carriers. *Nat Cell Biol* 2014; **16**: 592.
35. Wu J, Lu M, Li Y, *et al*. Regulation of a TGF- β 1–CD147 self-sustaining network in the differentiation plasticity of hepatocellular carcinoma cells. *Oncogene* 2016; **35**: 5468–5479.
36. Lau KS, Partridge EA, Grigorian A, *et al*. Complex N-glycan number and degree of branching cooperate to regulate cell proliferation and differentiation. *Cell* 2007; **129**: 123–134.
37. Guo H, Johnson H, Randolph M, *et al*. Specific posttranslational modification regulates early events in mammary carcinoma formation. *Proc Natl Acad Sci U S A* 2010; **107**: 21116–21121.
38. Thiery JP, Acloque H, Huang RYJ, *et al*. Epithelial–mesenchymal transitions in development and disease. *Cell* 2009; **139**: 871–890.
39. Xu Q, Akama R, Isaji T, *et al*. Wnt/ β -catenin signaling down-regulates N-acetylglucosaminyltransferase III expression. *J Biol Chem* 2011; **286**: 4310–4318.
40. Maupin KA, Sinha A, Eugster E, *et al*. Glycogene expression alterations associated with pancreatic cancer epithelial–mesenchymal transition in complementary model systems. *PLoS One* 2010; **5**: e13002.
41. Terao M, Ishikawa A, Nakahara S, *et al*. Enhanced epithelial–mesenchymal transition-like phenotype in N-acetylglucosaminyltransferase V transgenic mouse skin promotes wound healing. *J Biol Chem* 2011; **286**: 28303–28311.
42. Kamada Y, Mori K, Matsumoto H, *et al*. N-Acetylglucosaminyltransferase V regulates TGF- β response in hepatic stellate cells and the progression of steatohepatitis. *Glycobiology* 2012; **22**: 778–787.
43. Li N, Xu H, Fan K, *et al*. Altered β 1,6-GlcNAc branched N-glycans impair TGF- β -mediated epithelial-to-mesenchymal transition through Smad signalling pathway in human lung cancer. *J Cell Mol Med* 2014; **18**: 1975–1991.
44. Kato N, Yuzawa Y, Kosugi T, *et al*. The E-selectin ligand basigin/CD147 is responsible for neutrophil recruitment in renal ischemia/reperfusion. *J Am Soc Nephrol* 2009; **20**: 1565–1576.
45. Kiermaier E, Moussion C, Veldkamp CT, *et al*. Polysialylation controls dendritic cell trafficking by regulating chemokine recognition. *Science* 2016; **351**: 186–190.

46. Cai X, Thinn A, Wang Z, *et al.* The importance of *N*-glycosylation on $\beta 3$ integrin ligand binding and conformational regulation. *Sci Rep* 2017; **7**: 4656.
47. Li Y, Wu J, Song F, *et al.* Extracellular membrane-proximal domain of HAb18G/CD147 binds to metal ion-dependent adhesion site (MIDAS) motif of integrin $\beta 1$ to modulate malignant properties of hepatoma cells. *J Biol Chem* 2012; **287**: 4759–4772.
48. Hou S, Hang Q, Isaji T, *et al.* Importance of membrane-proximal *N*-glycosylation on integrin $\beta 1$ in its activation and complex formation. *FASEB J* 2016; **30**: 4120–4131.
49. Xue G, Hemmings BA. PKB/Akt-dependent regulation of cell motility. *J Natl Cancer Inst* 2013; **105**: 393–404.
50. Tang J, Wu YM, Zhao P, *et al.* Overexpression of HAb18G/CD147 promotes invasion and metastasis via $\alpha 3\beta 1$ integrin mediated FAK-paxillin and FAK-PI3K-Ca²⁺ pathways. *Cell Mol Life Sci* 2008; **65**: 2933–2942.
51. Khan GJ, Gao Y, Gu M, *et al.* TGF- $\beta 1$ causes EMT by regulating *N*-acetyl glucosaminyl transferases via downregulation of non-muscle myosin II-A through JNK/P38/PI3K pathway in lung cancer. *Curr Cancer Drug Tar* 2017; **17**: 1–11.

SUPPLEMENTARY MATERIAL ONLINE

Supplementary figure legends

Figure S1. Confocal microscopy images of CD147 and $\beta 1,6$ -GlcNAc-branched *N*-glycans

Figure S2. Western blotting analysis of HAb18G/CD147 expression in HepG2 and Huh-7 cells treated with various concentrations of swainsonine for 48 h

Figure S3. Immunofluorescence of HEK293T cells transfected with WT-CD147-GFP and 3Q-CD147-GFP plasmids

Table S1. Antibody details

Table S2. shRNA and quantitative real-time PCR primer sequences

50 Years ago in the *Journal of Pathology*...

A comparison of the organisation and fate of autologous pulmonary emboli and of artificial plasma thrombi in the anterior chamber of the eye, in normocholesterolaemic rabbits

N. G. Ardlie and C. J. Schwartz

The follicular arterioles of the spleen in canine interstitial nephritis

Lindsay J. Anderson

The organisation and fate of autologous pulmonary emboli in hypercholesterolaemic rabbits

N. G. Ardlie and C. J. Schwartz

To view these articles, and more, please visit:

www.thejournalofpathology.com

Click 'ALL ISSUES (1892 - 2018)', to read articles going right back to Volume 1, Issue 1.

The Journal of Pathology
Understanding Disease

